HHS Public Access

Author manuscript

Sci Transl Med. Author manuscript; available in PMC 2017 March 21.

Published in final edited form as:

Sci Transl Med. 2016 September 21; 8(357): 357ra122. doi:10.1126/scitranslmed.aaf4823.

Inhibition of Ileal Bile Acid Uptake Protects Against Non-alcoholic Fatty Liver Disease in High Fat Diet-fed Mice

Anuradha Rao[1], **Astrid Kosters**[1], **Jamie E. Mells**[1], **Wujuan Zhang**[2], **Kenneth D. R. Setchell**[2], **Angelica M. Amanso**[1], **Grace M. Wynn**[1], **Tianlei Xu**[3], **Brad T. Keller**[4], **Hong Yin**[5], **Sophia Banton**[6], **Dean P. Jones**[6,7], **Hao Wu**[8], **Paul A. Dawson**[1,5], and **Saul J. Karpen**[1,5,#]

[1]Department of Pediatrics, Emory University School of Medicine, 1760 Haygood Drive NE, Atlanta GA 30322

[2]Department of Pathology and Laboratory Medicine, Cincinnati Children's Hospital Medical Center, 3333 Burnet Avenue, Cincinnati, OH 45229

[3]Department of Mathematics and Computer Science, Emory University, Atlanta, GA 30322

[4]Vasculox, Inc., St. Louis, MO 63108

[5]Children's Healthcare of Atlanta, 2015 Uppergate Drive NE Atlanta, GA 30322

[6]Department of Biochemistry, Emory University, 1510 Clifton Rd NE, Atlanta GA 30322

[7]Department of Medicine, Emory University School of Medicine, 100 Woodruff Circle, Atlanta, GA 30322

[8]Department of Biostatistics and Bioinformatics, Rollins School of Public Health, Emory University, Atlanta, GA 30322

[#]To whom correspondence should be addressed: Saul J. Karpen, M.D., Ph.D.; Raymond F. Schinazi Distinguished Biomedical Chair, Pediatric Gastroenterology, Hepatology and Nutrition, Emory University School of Medicine, Children's Healthcare of Atlanta, Health Sciences Research Building, 1760 Haygood Dr., NE, Ste. 204E, Atlanta, GA 30322. skarpen@emory.edu.

Materials and Methods

Author contributions: AR, AK, JEM, WZ, KS, TX, BTK, HY, GMW, AMA, SB, DPJ, and HW performed the experiments, collected, and analyzed the data; SJK and PAD managed and designed the study, conceived the experiments, and AK, AR, AMA, PAD and SJK wrote the manuscript.

Competing interests: The other authors declare that they have no competing interests.

Data and materials availability: *Asbt*$^{-/-}$ mice are available for purchase through Jackson Laboratories (Bar Harbor, ME). SC-435 was made available as a research gift from Shire Pharmaceuticals. RNA-Seq data are available through GEO (GSE84994).

Abstract

Non-alcoholic fatty liver disease (NAFLD) is the most common chronic liver disease in the Western world, and safe and effective therapies are needed. Bile acids (BAs) and their receptors (including the nuclear receptor for BAs, FXR) play integral roles in regulating whole body metabolism and hepatic lipid homeostasis. We hypothesized that interruption of the enterohepatic BA circulation using a luminally-restricted Apical Sodium-dependent BA Transporter (ASBT) inhibitor (ASBTi; SC-435) would modify signaling in the gut-liver axis and reduce steatohepatitis in high fat diet (HFD)-fed mice. Administration of this ASBTi increased fecal BA excretion and mRNA expression of BA synthesis genes in liver, and reduced mRNA expression of ileal BA-responsive genes, including the negative feedback regulator of BA synthesis, Fibroblast Growth Factor 15 (FGF15). ASBT inhibition resulted in a marked shift in hepatic BA composition, with a reduction in hydrophilic, FXR antagonistic species and an increase in FXR agonistic BAs. ASBT inhibition restored glucose tolerance, reduced hepatic triglyceride and total cholesterol concentrations, and improved NAFLD Activity Score (NAS) in HFD-fed mice. These changes were associated with reduced hepatic expression of lipid synthesis genes (including LXR target genes), and normalized expression of the central lipogenic transcription factor, *Srebp1c*. Accumulation of hepatic lipids and SREBP1 protein were markedly reduced in HFD-fed $Asbt^{-/-}$ mice, providing genetic evidence for a protective role mediated by interruption of the enterohepatic BA circulation. Taken together, these studies suggest that blocking ASBT function with a luminally-restricted inhibitor can improve both hepatic and whole body aspects of NAFLD.

One Sentence Summary

Inhibition of the ileal bile acid transporter treats multiple features of nonalcoholic steatohepatitis in high fat diet-fed mice.

Introduction

Non-alcoholic fatty liver disease (NAFLD) is one of the most common liver diseases in the Western world, with an increasing prevalence around the globe (1, 2). NAFLD encompasses a pathophysiological spectrum ranging from steatosis to nonalcoholic steatohepatitis (NASH), cirrhosis, and liver carcinoma, along with substantial liver and whole body metabolic derangements. Effective medical therapies to slow or reverse aspects of this progression are limited. Inadequate or no response was observed for pioglitazone, vitamin E, and omega 3 fatty acid in clinical trials for NASH, although a recent trial with the FXR agonistic bile acid (BA) analog obeticholic acid (OCA) showed promising results (3–6). Dysregulation of hepatic lipid, sterol, and insulin-mediated metabolism appear to be major pathophysiologic contributors, but an incomplete understanding of the mechanisms underlying development of NAFLD and its progression to NASH continue to impact the development of rational therapeutics.

BAs, their receptors (FXR, TGR5, and S1PR2), and gut luminal BA-metabolizing bacteria have emerged as important regulators of hepatic lipid and glucose metabolism (7–9). BAs are synthesized from cholesterol in the liver, secreted into bile as the major solute, and function to facilitate lipid absorption in the intestine. Approximately 95% of intestinal BAs

are reabsorbed in the ileum by the Apical Sodium-dependent BA Transporter (ASBT) and conveyed in the portal vein to the liver, where they are taken up by hepatocytes to be resecreted into bile (10). This efficient enterohepatic circulation serves to maintain the BA pool and predominantly restrict BAs to intestinal and hepatobiliary compartments. The size and composition of the BA pool is dependent upon many factors, including FXR-dependent feedback regulatory pathways in both liver and ileum, enterohepatic cycling frequency, and metabolism by gut microbiota (10, 11). Changes in compartmentalization, concentration, and composition of the BA pool may have metabolic regulatory consequences, particularly in light of the spectrum of FXR agonistic and antagonistic potencies possessed by individual BAs. However, confounding our understanding of the metabolic effects of BAs via FXR and other receptors is their complex relationship with the gut microbiota, whereby BA pool size and composition appear to be a major regulator of the microbiome community and vice versa (9).

BA signaling in the intestine and liver has a role in the regulation of lipid, glucose, and energy homeostasis and is a potential target for treatment of obesity and NAFLD (12, 13). However, the underlying mechanisms remain unclear, because interventions that increase, as well as those that decrease BA (and FXR) signaling may yield metabolic benefits (8, 14–20). In this study, we focused on examining the effects of pharmacologic and genetic inhibition of ileal BA absorption on the development of fatty liver in the American Lifestyle-Induced Obesity Syndrome (ALIOS) HFD-fed mouse model of NAFLD (21). Oral administration of SC-435, a potent luminally-restricted ASBT inhibitor (ASBTi), restored glucose tolerance, reduced the steatohepatitic pathology, and altered liver gene expression in HFD-fed mice. Analysis of potential mechanisms in this dietary model and in HFD-fed *Asbt*$^{-/-}$ mice revealed that the improved features of NAFLD correlated in part with reductions in expression of LXR target genes along with a shift towards a more hydrophobic and FXR agonistic profile of the hepatic BA pool.

Results

Administration of an ASBTi impairs ileal BA uptake in HFD-fed mice

To determine if interrupting the enterohepatic circulation of BAs with an ASBTi can improve HFD-induced hepatic steatosis, male C57Bl/6J mice were fed one of 4 diets for 16 weeks as outlined in Fig. 1A: chow, HFD (modified ALIOS: 45% kcal fat plus 0.2% w/w cholesterol), HFD plus ASBTi for 16 weeks (60 ppm SC-435, ~11 mg/kg/day; HFD/ASBTi16w), or HFD for 12 weeks followed by HFD/ASBTi for the final 4 weeks (HFD/ASBTi4w) to determine if the HFD-induced changes could be reversed. All HFD groups were given 4% sucrose water ad libitum (21). For clarity, data related to the 16-week arm are discussed first, followed by a section describing the final 4-week treatment arm. In agreement with previous studies (22–24) ileal BA absorption was impaired by administration of the ASBTi as indicated by a 4-fold increase in fecal BA excretion, induction of hepatic sentinel BA synthesis target genes *Cyp7a1* and *Cyp8b1* (by 2.4±1.0 fold, $P<0.0001$, and 2.3±1.0 fold, $P<0.0001$, respectively; see table S1 for P values), suppression of FXR-activated *Fgf15* mRNA expression in ileum (by 93±7%; $P<0.0001$), and increased FXR-responsive *Ibabp* mRNA expression in colon (7.0±2.0 fold; $P<0.0001$; Fig

1B–E). *Asbt* mRNA expression in ileum and colon was unchanged by administration of the ASBTi (Fig. S1A–B). In comparison to untreated HFD-fed mice, administration of the ASBTi induced colonic expression of *Akr1b7*, an FXR target gene involved in BA metabolism in mice (Fig. S1C). Thus, luminally-restricted inhibition of ASBT in HFD-fed mice showed the anticipated effects in ileum, colon, and liver with respect to BA metabolism. Because BAs have been reported to induce injury (25, 26) we also examined the colonic expression of genes involved in cell stress and oncogenic signaling. There were no differences between HFD and HFD/ASBTi16w mice in colonic expression of genes involved in ER stress (*Atf6, Ddit3, Hspa1a, Hspa1b, Xbp1, Xbp1p*; Fig. S1D), oncogenic signaling genes (*Cdkn2a, Ctnnb1, Ccnd1, Myc, Mmp7*, and *Ogg1*; Fig. S1E), or genes involved in innate immunity and inflammation (*Ccl2, Il1b, Il6, Il12a, Il12b, Tnf*; Fig. S1F).

Administration of an ASBTi restores glucose tolerance in HFD-fed mice

HFD feeding slightly increased final body weight compared to chow-fed mice, in agreement with the small increase in daily caloric intake (Fig. 2A–C). However, the final body weights of the HFD/ASBTi16w mice were not different from the HFD mice, despite consuming more calories each day (Fig. 2A–C, S1G–H). Liver weight to body weight ratio was increased in the HFD versus chow-fed mice, which was still apparent in the 16 week HFD/ASBTi treated group (Fig. 2D). Markers of hepatocellular injury such as serum ALT and AST were not different between the groups, but a minor increase in serum alkaline phosphatase was observed in the HFD but not HFD/ASBTi16w mice (Fig. S1I). To determine the effects of the ASBTi on glucose and systemic insulin sensitivity, we performed glucose and insulin tolerance tests. Feeding mice with the HFD for 16 weeks resulted in glucose intolerance, whereas addition of an ASBTi to the HFD during this entire time restored glucose tolerance and improved systemic insulin sensitivity (Fig. 2E–F, S2A–B).

Administration of an ASBTi prevents hepatic steatosis in HFD-fed mice

After 16 weeks of feeding mice with the HFD, many characteristic histological features of NASH were observed in the animals' livers, including steatosis, lobular inflammation, hepatocyte ballooning, and Mallory bodies (Fig. 3A–B). Compared to HFD-fed mice, lipid deposition was markedly decreased in the HFD/ASBTi16w mice and to a lesser extent in HFD/ASBTi4w mice (Fig. 3B–D). Blinded histologic assessment of slides by an experienced hepatopathologist (H.Y.) indicated that HFD/ASBTi16w treatment reduced the NAFLD Activity Score (NAS) (27) from 4.8±1.0 to 2.8±0.9, primarily driven by improvements in the Steatosis Score (Fig. 3E–F; see table S2 for individual components of the NAS). Biochemical lipid measurements confirmed severe triglyceride (TG) and cholesteryl ester deposition in livers of HFD-fed mice compared to chow-fed animals (~12 and 15-fold increases, respectively; Fig. 3G–H). The hepatic concentrations of TG, cholesteryl ester, and total cholesterol were markedly reduced in the HFD/ASBTi16w mice compared to HFD-fed mice, to a degree whereby the lipid content of HFD/ASBTi16w livers was similar to the liver lipid content in chow-fed mice (Fig. 3G–H, S2C). Only minor effects were noted for hepatic free cholesterol concentrations in diet and treatment groups when compared to chow (Fig. S2D). Liver fibrosis was also assessed, but neither histologic assessment by Sirius Red staining nor biochemical quantitation of hydroxyproline content

revealed any significant hepatic fibrosis in the HFD-fed mice. As such, there was little effect on these fibrosis markers in any of the treatment groups (Fig. S3).

Administration of an ASBTi alters hepatic BA pool composition and FXR-regulatory properties in HFD-fed mice

The total BA content was not different between chow, HFD, and ASBTi-treated livers (Fig. 4A), and HFD-feeding had no discernible impact upon hepatic BA pool composition when compared to chow (Fig. 4B–D). However, blocking intestinal BA uptake altered the hepatic BA pool composition (Fig. 4B), changing its chemical and predicted FXR signaling properties. Ileal ASBT inhibition reduced the hepatic concentration of 6-hydroxylated TMCA species (ω, α, and β by > 50%) and increased the amount of the more hydrophobic BAs, TCDCA and TDCA, by greater than 10-fold (Fig. 4B). As a result, the hepatic BA content shifted from a typical ~0.8:1 balanced ratio of non-6-hydroxylated to 6-hydroxylated) BA species in chow and HFD-fed mice, to a >4:1 ratio with a predominance of the non-6-hydroxylated species in the livers of ASBTi mice (Fig. 4B). This is reflected by an increase in the calculated hydrophobicity index, which rose from −0.406 to +0.088 (Fig. 4C). In addition to changing the physicochemical properties of the hepatic BA pool, administration of the ASBTi also yielded a BA pool predicted to be, in sum, substantially more FXR agonistic (16, 28–30) (Fig. 4B, 4D). Because FXR-signaling BAs are important physiological regulators of multiple hepatic functions including lipid metabolism, the combined amounts of FXR agonistic (TCA, TCDCA, TDCA, TLCA, CA) and antagonistic (MCAs) BA species were compared to the hepatic TG and cholesterol content in livers of individual HFD, HFD/ASBTi16w, and HFD/ASBTi4w mice. Hepatic TG and cholesterol content directly correlated with amount of FXR antagonistic muricholates (r = 0.4980, P = 0.0023; r= 0.5829, P = 0.0002) and inversely correlated with TCDCA+TDCA content (r = −0.5381, P = 0.0009; r = −0.5630, P = 0.0004) (Fig. S4). Overall, the marked alteration of the hepatic BA pool towards FXR agonism correlated with the histologic and biochemical improvements driven by pharmacological inhibition of ileal ASBT function.

Previous in vitro studies using primarily individual BAs found TCDCA and TDCA to be potent FXR agonists, whereas TUDCA and TMCA species failed to activate FXR and may function as FXR antagonists (16, 30–32). To begin modeling the FXR activity of the distinct hepatic BA pools in HFD and HFD/ASBTi mice, we examined the ability of BA mixtures to activate an FXR reporter plasmid in transfected human liver-derived HepG2 cells. In vitro, βTMCA antagonizes FXR activation by TCA or TCDCA (Fig. 4E–F). However, given the in vivo findings, we thought it relevant to examine the in vitro FXR antagonistic properties of the muricholates in more complex mixtures of BAs, paralleling the composition of BAs present in liver. Mixtures of the 6 most abundant taurine-conjugated BAs were reconstituted at the ratios present in HFD or HFD/ASBTi livers (Fig. 4B, table S3) to model the in vivo exposure to multiple BAs and their combined effect on FXR activity. The BA composition present in HFD/ASBTi livers activated the FXR reporter plasmid to a greater extent than the reconstituted BA mixture from HFD livers (Fig. 4G). These studies suggest that the consequences of this marked shift in liver BA composition may underlie some of the hepatic responses to ileal ASBT inhibition.

Administration of an ASBTi alters hepatic metabolic gene expression in HFD-fed mice

To explore the gene-regulatory mechanisms underlying the hepatic effects of the luminally-active ASBTi on HFD-fed mice, we performed RNA-seq analyses using livers from mice fed chow, HFD, and HFD/ASBTi16w. Comparison of the chow and HFD groups identified 5033 RNA species that were differentially expressed in livers of HFD-fed mice (Fig. 5A, S5A; 3186 genes upregulated and 1847 genes downregulated; $P<0.05$, table S4). Subsequent comparison of liver gene expression in HFD versus HFD/ASBTi16w mice identified 1483 differentially expressed genes (764 genes upregulated and 719 downregulated; $P<0.05$) (Fig. 5A; table S4). Cross-comparison of the lists of genes differentially expressed in chow versus HFD mice and in HFD versus HFD/ASBTi16w mice revealed 675 genes common to the 2 data sets. For 650 of these genes (96%), ASBTi treatment of the HFD mice changed their expression towards levels seen in chow-fed mouse livers, including several key genes involved in fatty acid and cholesterol metabolism (*Srebp1c, Srebp2, Abcg5, Abcg8*, and *Cidec*; Fig. 5A–B, table S4). Hierarchical clustering of RNA expression and ontological and pathway analyses revealed markedly distinct patterns between groups (Fig. 5B–C, S5B–C), confirming major changes in hepatic gene expression induced both by HFD and subsequently by ileal ASBT inhibition. Administration of the ASBTi changed hepatic gene expression in a variety of lipid, fatty acid, and cholesterol metabolic pathways, as well as intracellular transport and signaling (Fig. 5C, table S4). Taken together, these RNA-seq studies indicate marked shifts in hepatic gene transcription, intracellular signaling, and metabolism in HFD-fed mice as a consequence of ileal ASBT inhibition.

Real-time PCR was used to measure expression of critical genes in a variety of NAFLD-related pathways in the liver as well as the ileum and colon, with the analyses focused primarily upon HFD versus HFD/ASBTi16w mice (Fig. 6A–C, S6A–E). With regard to BA signaling, differential effects were observed for several of the known hepatic FXR target genes including *Abcb11* and *Shp*, whereas mRNA expression of the BA-activated G-protein coupled receptor (GPCR) sphingosine-1-phosphate receptor 2 (*S1pr2*) and its downstream target sphingosine kinase 2 (*Sphk2*) were increased 2–3 fold in HFD-fed mice and reduced by 50% with ASBT inhibition (Fig. 6A). Expression of FXR target genes was generally lower in ileum and increased in colon (Fig. 1D–E, 6B–C), reflecting the block in ileal BA absorption. Expression of the BA-activated GPCR *Tgr5* was unaffected in liver, ileum, or colon by administration of the ASBTi (Fig. 6A–C). There were no changes in ileal or colonic expression of the TGR5 target gene *Gcg*, the GLP-1 precursor (Fig. S6B–C).

The increases in hepatic BA synthesis with inhibition of the ileal ASBT resulted in the expected compensatory increase in expression of cholesterol biosynthetic genes (*Srepb2, Hmgr*; Fig. 6A), and the reduced hepatic cholesterol content in HFD/ASBTi16w mice was associated with lower expression of *Ch25oh* (an endogenous source of the LXRα ligand, 25-hydroxycholesterol) and LXRα target genes (*Abcg5, Abcg8, and Srebp1c*). Inhibition of ileal ASBT also markedly altered the expression of hepatic genes involved in fatty acid and TG metabolism. Expression of a variety of key biosynthetic and regulatory genes (*Srebp1c, Scd1, Fads1, Fads2, and Pparg*,) was increased 2–4 fold by HFD, and all were reduced toward chow-fed levels with ASBT inhibition (Fig. 6A, S6D). Fatty acid oxidation gene expression was minimally affected by the ASBTi (*Fgf21, Ppara, Acaa1b*; Fig. 6A, S6D). In

line with histological data and changes in lipogenic gene expression, RNA levels of lipid droplet formation genes *Cidea* and *Fsp27/Cidec* were induced >50-fold by HFD and reduced by 70±30% and 86±10% with the ASBTi (Fig. 6A; S6E).

The presence of inflammation and fibrosis with steatosis are hallmarks of progression to NASH, and HFD-induced pro-inflammatory gene expression (*Tnf, Il1b, Ccl2, Cxcl9, Cxcl10*) was reduced in the presence of the ASBTi, whereas mRNA expression of *Lcn2*, a small secreted adipokine with a protective role in hepatic inflammation, was induced (Fig. 6A; S6E). RNA expression of fibrosis genes *Col1a1, Msln*, and *Gli2* were increased by HFD and reduced to baseline with ASBT inhibition, suggesting an anti-fibrotic effect of the ASBTi (Fig. 6A, S6E), although there was no significant fibrosis detected in any of the experimental conditions in this study (Fig. S3). Altogether, 16 weeks of ileal ASBT inhibition resulted in substantial alterations in gene expression in livers of mice fed HFD, related principally to BA, cholesterol, and fatty acid metabolism, but also to a reduction in markers of inflammation and response to stress.

Administration of an ASBTi does not alter ceramides in HFD-fed mouse ileum or liver

Recent studies in a different HFD-fed mouse model (8, 18) support a role for ileal FXR signaling-associated changes in ceramide synthesis and secretion into the portal circulation in the development of fatty liver and obesity-related metabolic dysfunction. However, targeted mass spectrometry analysis of both liver and ileal ceramide concentrations in response to HFD or HFD/ASBTi16w revealed no significant changes in the amounts of total ceramide or individual ceramide species in either tissue (Fig. S7). These findings suggest that different mechanisms are operative in this model, where the ASBTi blocks both ileal FXR signaling and ileal BA internalization.

Administration of an ASBTi partially reverses established NAFLD after 12 weeks of HFD

To determine if inhibition of ileal BA uptake also impacts established NAFLD, mice were fed the HFD for 12 weeks followed by 4 weeks of HFD/ASBTi. The responses of sentinel FXR-responsive genes in the liver, intestine, and colon were similar in the 4 and 16-week ASBTi treatments (Fig. 1C–E). This short treatment period induced some changes not seen in the full 16 week treatment, such as reducing the liver/body weight ratio (Fig. 2D), but glucose tolerance, NAS, and steatosis score were not significantly affected (Fig. 2E–F, 3E–F) in HFD/ASBTi4w compared to HFD mice. However, hepatic TG and cholesterol contents were dramatically reduced compared to HFD-fed mice (Fig. 3G–H, S2C) and visually, there appeared to be zonally-restricted reductions in lipid deposition with the HFD/ASBTi4w treatment (Fig. 3B and 3D). In addition, hepatic BA composition was similarly altered with 4 weeks of ASBTi as with 16 weeks of treatment (Fig. 4B–D). Overall these results indicate a partial reversal of the hepatic effects of 12 weeks of HFD by ASBTi treatment during the ensuing 4 weeks of HFD.

Asbt$^{-/-}$ mice are resistant to hepatic steatosis with short-term HFD feeding

To confirm these findings and explore potential mechanisms involving the role of ASBT in the hepatic response to HFD, short-term (1w) HFD was administered to *Asbt*$^{-/-}$ and WT (*Asbt*$^{+/+}$) mice followed by histologic, biochemical, and molecular analyses of the liver and

ileum. After 1 week of HFD, when compared to WT mice, *Asbt*$^{-/-}$ mice gained less weight, despite ingesting essentially the same amount of calories as WT mice (Fig. 7A–B). Similarly, liver weight in HFD-fed *Asbt*$^{-/-}$ mice was reduced compared to HFD-fed WT mice (Fig. 7C), but liver weight:body weight ratios were unchanged (Fig. 7D). Histological and biochemical analyses showed that the livers of HFD-fed *Asbt*$^{-/-}$ mice, but not the livers of WT mice, were protected against lipid accumulation after 1 week of HFD (Fig. 7E–L).

Asbt$^{-/-}$ mice have reduced total hepatic BAs, with a BA composition similar to those treated with ASBTi

Unlike in mice treated with the luminally-restricted ASBTi, total hepatic BA content was reduced in *Asbt*$^{-/-}$ mice (by ~50%, Fig. 8A). However, the hepatic BA compositional changes were similar in both models (Fig. 4B and 8B), shifting towards a more hydrophobic, FXR agonistic pool (Fig. 8C–D). Gene expression consequences of 1 week of HFD in *Asbt*$^{-/-}$ mouse livers were notable for changes similar to those seen in the longer-term ASBTi treatments (Fig. 8E; S8). Of note for BA and cholesterol metabolism, *Cyp7a1* mRNA was increased ~5-fold, expression of BA-regulated genes (*Shp, Abcb11, Mafg*) was reduced in HFD-fed *Asbt*$^{-/-}$ mice, and the downregulation of *Hmgr* and *Srebp2* mRNA observed in the HFD-fed WT mice was blocked in HFD-fed *Asbt*$^{-/-}$ mice. Increases in lipid metabolism-associated genes (*Abcg8, Lxra, Srebp1c, Scd1, Ppara, Ehhadh*) in HFD-fed WT mice were abrogated in HFD-fed *Asbt*$^{-/-}$ mice (Fig. 8E; S8), comparable to changes induced by ASBT inhibition. Immunoblot analysis showed that the amount of liver SREBP1 protein increased after 1 week of HFD feeding in WT mice (P=0.0084) but not in *Asbt*$^{-/-}$ mice (P=0.913; Fig. 8F). Thus, absence of ASBT function markedly impairs the accretion of features of NAFLD in mice in as short a time period as 1 week of HFD, and engages pathways associated with a more FXR agonistic hepatic BA pool. Taken together, the alterations in liver BA composition, ileal and colonic gene expression, hepatic TG and cholesterol content, and resolution of insulin resistance support inhibition of ileal ASBT function as a rational target for the hepatic and metabolic consequences of diet-induced fatty liver.

Discussion

In the current study of a mouse model of HFD-induced NASH, the presence of a minimally-absorbable specific inhibitor of intestinal BA uptake (ASBTi) prevented hepatic accumulation of TGs and cholesterol and restored whole body insulin sensitivity. Ileal ASBT inhibition in HFD-fed mice was associated with substantial hepatic transcriptional and metabolic re-programming, suggesting that hepatocellular BA signaling was markedly altered by this gut-restricted pharmacological intervention. Ileal ASBT inhibition prevented hepatic cholesterol accumulation by inducing BA biosynthesis from cholesterol stores, and shifting the liver BA pool composition towards one enriched in hydrophobic species that are more FXR agonistic in nature. This included a dramatic reduction in hydrophilic, FXR antagonistic tauromuricholates (16, 30) associated with increases in TCDCA, TDCA, and other FXR agonistic BAs. The reduction in muricholates is likely due to decreases in CDCA synthesis via the alternative pathway secondary to reductions in hepatic cholesterol content and to suppression of hepatic 6-hydroxylation. Hepatic TG and cholesterol content directly

correlated with the amount of FXR antagonistic muricholates and inversely correlated with the amount of FXR agonist TCDCA+TDCA in the liver. Similar decreases in hepatic lipid accretion were observed in *Asbt*$^{-/-}$ mice versus WT mice with short-term HFD-feeding, and in the hepatic BA composition of the *Asbt*$^{-/-}$ mice, regardless of diet. Exposure of transfected HepG2 cells to synthetic BA mixtures modeling the hepatic BA composition found in ileal ASBT-inhibited mice increased the activation of an FXR luciferase reporter plasmid, as compared to the hepatic BA composition of HFD mice. Taken together, the findings in this study suggest that inhibition of ileal BA uptake has meaningful biological and gene regulatory consequences that address multiple features of NASH in mice.

Ileal ASBT inhibition resulted in profound reduction in hepatic lipids, improvement in insulin sensitivity, and alterations in the expression of hepatic lipid, inflammatory, and BA regulatory genes. The underlying mechanisms may relate to alterations in BA, FXR, or LXR signaling, or other pathways. Recent work by Jiang et al (8, 18). demonstrated that intestinal-specific inactivation or inhibition of FXR produced metabolic benefit by reducing the intestinal production of bioactive ceramides, which promote fatty liver and obesity-related metabolic dysfunction in HFD-fed mice. In the present study, inhibition of ileal FXR activation was associated with metabolic benefit without a change in ileal or hepatic ceramide content, suggesting alternative mechanisms leading to improvements in NASH. These differential results may be related to consequences of specifically targeting FXR versus BA-mediated signaling. For example, with regard to the ileal enterocyte, inhibition or inactivation of ASBT blocks BA internalization, and is predicted to cause a pan-inhibition of FXR as well as other intercellular BA targets and signaling pathways. This is in contrast to intestinal-specific inactivation of FXR or administration of intestinally-selective FXR antagonists, both of which would block only the FXR signaling component. A relevant confounder to focusing upon inhibiting of intestinal FXR signaling to improve NASH is recent work by Fang et al that demonstrated improved lipid handling and NASH in mice with a gut-restricted FXR agonist (17). Thus with regard to NASH in mice, the beneficial effects associated with modifying BA signaling in ileal enterocytes may involve FXR and non-FXR targets as well as ceramide and non-ceramide pathways, whose relative contributions remain to be determined.

Several metabolic pathways are involved in maintaining hepatic lipid homeostasis, whereby dysregulation of each can result in accumulation of lipid droplets. It is well established that lipid and TG syntheses are increased in NAFLD (33). In addition, changes in BA composition can elicit major effects on regulation of metabolic pathways in liver (14, 30, 34, 35). Indeed, hepatic expression of genes involved in lipid synthesis and lipid droplet formation were induced after 16 weeks of HFD, and reduced in the presence of the ASBTi. In contrast, there was little effect on gene expression for beta-oxidation or lipoprotein secretion pathways in this study, suggesting that they did not play a major role in the changes in hepatic TG content in this model. It is important to note that the modified ALIOS diet used in this study contained a modest amount of added (0.2% w/w) cholesterol, and cholesterol accumulation is a likely contributor to NASH (36–40). Cholesterol accumulation may cause increases in hepatic inflammation and oxysterol-mediated alterations in gene expression, mostly via LXRα target genes including *Srebp1c*. Additional studies are needed to explore the hepatic consequences of reducing cholesterol and cholesterol-derived

metabolites (such as oxysterols) and whether this is an important determinant of the improvements in response to an ASBTi. Thus, the mechanisms mediating the effects of ASBT inhibition may extend beyond FXR mediated signaling in animal models of NAFLD.

Although adding an ASBTi for the final 4 weeks of the 16-week HFD treatment altered the hepatic BA composition, it did not produce a histological improvement in NASH. The effects were intermediate, with similar decreases in hepatic TG and cholesterol accumulation as observed with 16-week treatment, but not some of the other metabolic and transcriptional effects. It is not clear if this was a result of an insufficient duration of treatment or whether the changes in BA metabolism and signaling induced by the ASBTi are insufficient to impact NASH once it is established. Additional studies using longer periods of intervention and other models of NASH will be required to answer these questions.

In summary, treatment of mice with a luminally-restricted ileal ASBT inhibitor markedly improved several facets of NASH and insulin resistance by engaging multiple components of BA signaling within the gut-liver axis. The finding that hepatic BA composition became more FXR agonistic in response to inhibition of ileal ASBT is likely to be mechanistically important, but may explain only a portion of the positive effects of ASBT inhibition observed in this mouse NASH model. There is also the question of whether these BA compositional changes are relevant for humans, who largely lack 6-hydroxylated BAs under most physiological conditions. However, the targeting of ileal BA uptake to alter liver FXR agonism may alleviate some of the concerns seen in the recent human NASH trial of a potent FXR agonist OCA which improved histological features of NASH, but also increased pro-atherogenic serum lipid concentrations in some subjects (6). Both surgical ileal exclusion and interruption of ileal BA uptake by pharmacological means have been shown to reduce serum LDL cholesterol by increasing hepatic cholesterol conversion to BAs (22, 41), so it is intriguing to speculate that inhibition of ASBT may provide a means to improve features of hepatic lipotoxicity and metabolic syndrome while alleviating some atherosclerotic risk factors. Mechanistic pre-clinical studies in addition to well-controlled human trials are needed to determine if these data in a mouse NASH model will translate to humans affected by NASH, and the long-term effects of such an intervention.

Materials and Methods

See supplementary file for materials and methods.

Supplementary Material

Refer to Web version on PubMed Central for supplementary material.

Acknowledgments

The authors would like to thank Lumena/Shire for the generous gift of SC-435, Dr. Dmitry Shayakhmetov and Dr. Nelson C. Di Paolo (Emory University, School of Medicine) for assistance and use of their microscope, the Yerkes Nonhuman Primate Genomics Core (Emory University, School of Medicine) for performing RNA-sequencing, Children’s Healthcare of Atlanta Pathology services for processing histology tissues, and Dr. Tim Osborne and Peter Phelan (Sanford Burnham Prebys Medical Discovery Institute) for assistance with SREBP1 immunoblotting.

Funding: The studies were supported by NIH (DK56239 SJK; DK047987 PAD; ES023485, AG038746, HL113451, ES019776, ES025632, EY022618, HD075784, HL095479, HL086773, HL125042 DPJ). JEM was supported by an NIH Fellowship in Research and Science Teaching (FIRST) Institutional Research and Academic Career Development Award (K12 GM000680). SJK and PAD were also supported by the Center for Transplantation and Immune-Mediated Disorders and Children's Healthcare of Atlanta.

BTK was an employee of Lumena Pharmaceuticals, now part of Shire Pharmaceuticals. PAD had previously served as a consultant for Lumena Pharmaceuticals.

References and notes

1. Loomba R, Sanyal AJ. The global NAFLD epidemic. Nature reviews. Gastroenterology & hepatology. 2013; 10:686–690. [PubMed: 24042449]
2. Younossi ZM, Koenig AB, Abdelatif D, Fazel Y, Henry L, Wymer M. Global epidemiology of nonalcoholic fatty liver disease-Meta-analytic assessment of prevalence, incidence, and outcomes. Hepatology. 2016; 64:73–84. [PubMed: 26707365]
3. Sanyal AJ, Chalasani N, Kowdley KV, McCullough A, Diehl AM, Bass NM, Neuschwander-Tetri BA, Lavine JE, Tonascia J, Unalp A, Van Natta M, Clark J, Brunt EM, Kleiner DE, Hoofnagle JH, Robuck PR, Nash CRN. Pioglitazone, vitamin E, or placebo for nonalcoholic steatohepatitis. The New England journal of medicine. 2010; 362:1675–1685. [PubMed: 20427778]
4. Nie B, Park HM, Kazantzis M, Lin M, Henkin A, Ng S, Song S, Chen Y, Tran H, Lai R, Her C, Maher JJ, Forman BM, Stahl A. Specific bile acids inhibit hepatic fatty acid uptake in mice. Hepatology. 2012; 56:1300–1310. [PubMed: 22531947]
5. Kim JK, Lee KS, Lee DK, Lee SY, Chang HY, Choi J, Lee JI. Omega-3 polyunsaturated fatty acid and ursodeoxycholic acid have an additive effect in attenuating diet-induced nonalcoholic steatohepatitis in mice. Experimental & molecular medicine. 2014; 46:e127. [PubMed: 25523099]
6. Neuschwander-Tetri BA, Loomba R, Sanyal AJ, Lavine JE, Van Natta ML, Abdelmalek MF, Chalasani N, Dasarathy S, Diehl AM, Hameed B, Kowdley KV, McCullough A, Terrault N, Clark JM, Tonascia J, Brunt EM, Kleiner DE, Doo E. N. C. R. Network. Farnesoid X nuclear receptor ligand obeticholic acid for non-cirrhotic, non-alcoholic steatohepatitis (FLINT): a multicentre, randomised, placebo-controlled trial. Lancet. 2015; 385:956–965. [PubMed: 25468160]
7. Mueller M, Thorell A, Claudel T, Jha P, Koefeler H, Lackner C, Hoesel B, Fauler G, Stojakovic T, Einarsson C, Marschall HU, Trauner M. Ursodeoxycholic acid exerts farnesoid X receptor-antagonistic effects on bile acid and lipid metabolism in morbid obesity. Journal of hepatology. 2015; 62:1398–1404. [PubMed: 25617503]
8. Jiang C, Xie C, Li F, Zhang L, Nichols RG, Krausz KW, Cai J, Qi Y, Fang ZZ, Takahashi S, Tanaka N, Desai D, Amin SG, Albert I, Patterson AD, Gonzalez FJ. Intestinal farnesoid X receptor signaling promotes nonalcoholic fatty liver disease. The Journal of clinical investigation. 2015; 125:386–402. [PubMed: 25500885]
9. Schnabl B, Brenner DA. Interactions between the intestinal microbiome and liver diseases. Gastroenterology. 2014; 146:1513–1524. [PubMed: 24440671]
10. Dawson PA, Karpen SJ. Intestinal transport and metabolism of bile acids. Journal of lipid research. 2015; 56:1085–1099. [PubMed: 25210150]
11. Chiang JY. Bile acid metabolism and signaling. Comprehensive Physiology. 2013; 3:1191–1212. [PubMed: 23897684]
12. Arab JP, Karpen SJ, Dawson PA, Arrese M, Trauner M. Bile acids & nonalcoholic fatty liver disease: Molecular insights and therapeutic perspectives. Hepatology. 2016 Jun 30. [Epub ahead of print] Review. PMID: 27358174.
13. Fuchs C, Claudel T, Trauner M. Bile acid-mediated control of liver triglycerides. Seminars in liver disease. 2013; 33:330–342. [PubMed: 24222091]
14. Watanabe M, Horai Y, Houten SM, Morimoto K, Sugizaki T, Arita E, Mataki C, Sato H, Tanigawara Y, Schoonjans K, Itoh H, Auwerx J. Lowering bile acid pool size with a synthetic farnesoid X receptor (FXR) agonist induces obesity and diabetes through reduced energy expenditure. The Journal of biological chemistry. 2011; 286:26913–26920. [PubMed: 21632533]
15. Prawitt J, Abdelkarim M, Stroeve JH, Popescu I, Duez H, Velagapudi VR, Dumont J, Bouchaert E, van Dijk TH, Lucas A, Dorchies E, Daoudi M, Lestavel S, Gonzalez FJ, Oresic M, Cariou B,

Kuipers F, Caron S, Staels B. Farnesoid X receptor deficiency improves glucose homeostasis in mouse models of obesity. Diabetes. 2011; 60:1861–1871. [PubMed: 21593203]

16. Li F, Jiang C, Krausz KW, Li Y, Albert I, Hao H, Fabre KM, Mitchell JB, Patterson AD, Gonzalez FJ. Microbiome remodelling leads to inhibition of intestinal farnesoid X receptor signalling and decreased obesity. Nature communications. 2013; 4:2384.
17. Fang S, Suh JM, Reilly SM, Yu E, Osborn O, Lackey D, Yoshihara E, Perino A, Jacinto S, Lukasheva Y, Atkins AR, Khvat A, Schnabl B, Yu RT, Brenner DA, Coulter S, Liddle C, Schoonjans K, Olefsky JM, Saltiel AR, Downes M, Evans RM. Intestinal FXR agonism promotes adipose tissue browning and reduces obesity and insulin resistance. Nature medicine. 2015; 21:159–165.
18. Jiang C, Xie C, Lv Y, Li J, Krausz KW, Shi J, Brocker CN, Desai D, Amin SG, Bisson WH, Liu Y, Gavrilova O, Patterson AD, Gonzalez FJ. Intestine-selective farnesoid X receptor inhibition improves obesity-related metabolic dysfunction. Nature communications. 2015; 6:10166.
19. Watanabe M, Morimoto K, Houten SM, Kaneko-Iwasaki N, Sugizaki T, Horai Y, Mataki C, Sato H, Murahashi K, Arita E, Schoonjans K, Suzuki T, Itoh H, Auwerx J. Bile acid binding resin improves metabolic control through the induction of energy expenditure. PloS one. 2012; 7:e38286. [PubMed: 22952571]
20. Ryan KK, Tremaroli V, Clemmensen C, Kovatcheva-Datchary P, Myronovych A, Karns R, Wilson-Perez HE, Sandoval DA, Kohli R, Backhed F, Seeley RJ. FXR is a molecular target for the effects of vertical sleeve gastrectomy. Nature. 2014; 509:183–188. [PubMed: 24670636]
21. Tetri LH, Basaranoglu M, Brunt EM, Yerian LM, Neuschwander-Tetri BA. Severe NAFLD with hepatic necroinflammatory changes in mice fed trans fats and a high-fructose corn syrup equivalent. American journal of physiology. Gastrointestinal and liver physiology. 2008; 295:G987–G995. [PubMed: 18772365]
22. Bhat BG, Rapp SR, Beaudry JA, Napawan N, Butteiger DN, Hall KA, Null CL, Luo Y, Keller BT. Inhibition of ileal bile acid transport and reduced atherosclerosis in apoE−/− mice by SC-435. Journal of lipid research. 2003; 44:1614–1621. [PubMed: 12810816]
23. Miethke AG, Zhang W, Simmons J, Taylor AE, Shi T, Shanmukhappa SK, Karns R, White S, Jegga AG, Lages CS, Nkinin S, Keller BT, Setchell KD. Pharmacological inhibition of apical sodium-dependent bile acid transporter changes bile composition and blocks progression of sclerosing cholangitis in multidrug resistance 2 knockout mice. Hepatology. 2016; 63:512–523. [PubMed: 26172874]
24. Baghdasaryan A, Fuchs CD, Osterreicher CH, Lemberger UJ, Halilbasic E, Pahlman I, Graffner H, Krones E, Fickert P, Wahlstrom A, Stahlman M, Paumgartner G, Marschall HU, Trauner M. Inhibition of intestinal bile acid absorption improves cholestatic liver and bile duct injury in a mouse model of sclerosing cholangitis. Journal of hepatology. 2016; 64:674–681. [PubMed: 26529078]
25. Sears CL, Garrett WS. Microbes, microbiota, and colon cancer. Cell host & microbe. 2014; 15:317–328. [PubMed: 24629338]
26. Barrasa JI, Olmo N, Lizarbe MA, Turnay J. Bile acids in the colon, from healthy to cytotoxic molecules. Toxicology in vitro : an international journal published in association with BIBRA. 2013; 27:964–977. [PubMed: 23274766]
27. Brunt EM, Kleiner DE, Wilson LA, Belt P, Neuschwander-Tetri BA. N. C. R. Network. Nonalcoholic fatty liver disease (NAFLD) activity score and the histopathologic diagnosis in NAFLD: distinct clinicopathologic meanings. Hepatology. 2011; 53:810–820. [PubMed: 21319198]
28. Klaassen CD, Cui JY. Review: Mechanisms of How the Intestinal Microbiota Alters the Effects of Drugs and Bile Acids. Drug metabolism and disposition: the biological fate of chemicals. 2015; 43:1505–1521. [PubMed: 26261286]
29. Parks DJ, Blanchard SG, Bledsoe RK, Chandra G, Consler TG, Kliewer SA, Stimmel JB, Willson TM, Zavacki AM, Moore DD, Lehmann JM. Bile acids: natural ligands for an orphan nuclear receptor. Science. 1999; 284:1365–1368. [PubMed: 10334993]
30. Sayin SI, Wahlstrom A, Felin J, Jantti S, Marschall HU, Bamberg K, Angelin B, Hyotylainen T, Oresic M, Backhed F. Gut microbiota regulates bile acid metabolism by reducing the levels of

tauro-beta-muricholic acid, a naturally occurring FXR antagonist. Cell metabolism. 2013; 17:225–235. [PubMed: 23395169]

31. Howard WR, Pospisil JA, Njolito E, Noonan DJ. Catabolites of cholesterol synthesis pathways and forskolin as activators of the farnesoid X-activated nuclear receptor. Toxicology and applied pharmacology. 2000; 163:195–202. [PubMed: 10698678]
32. Schaap FG, Trauner M, Jansen PL. Bile acid receptors as targets for drug development. Nature reviews. Gastroenterology & hepatology. 2014; 11:55–67. [PubMed: 23982684]
33. Duarte JA, Carvalho F, Pearson M, Horton JD, Browning JD, Jones JG, Burgess SC. A high-fat diet suppresses de novo lipogenesis and desaturation but not elongation and triglyceride synthesis in mice. Journal of lipid research. 2014; 55:2541–2553. [PubMed: 25271296]
34. Haeusler RA, Pratt-Hyatt M, Welch CL, Klaassen CD, Accili D. Impaired generation of 12-hydroxylated bile acids links hepatic insulin signaling with dyslipidemia. Cell metabolism. 2012; 15:65–74. [PubMed: 22197325]
35. Boesjes M, Bloks VW, Hageman J, Bos T, van Dijk TH, Havinga R, Wolters H, Jonker JW, Kuipers F, Groen AK. Hepatic farnesoid X-receptor isoforms alpha2 and alpha4 differentially modulate bile salt and lipoprotein metabolism in mice. PloS one. 2014; 9:e115028. [PubMed: 25506828]
36. Farrell GC, van Rooyen D. Liver cholesterol: is it playing possum in NASH? American journal of physiology. Gastrointestinal and liver physiology. 2012; 303:G9–G11. [PubMed: 22556144]
37. Savard C, Tartaglione EV, Kuver R, Haigh WG, Farrell GC, Subramanian S, Chait A, Yeh MM, Quinn LS, Ioannou GN. Synergistic interaction of dietary cholesterol and dietary fat in inducing experimental steatohepatitis. Hepatology. 2013; 57:81–92. [PubMed: 22508243]
38. Van Rooyen DM, Farrell GC. SREBP-2: a link between insulin resistance, hepatic cholesterol, and inflammation in NASH. Journal of gastroenterology and hepatology. 2011; 26:789–792. [PubMed: 21488942]
39. Van Rooyen DM, Gan LT, Yeh MM, Haigh WG, Larter CZ, Ioannou G, Teoh NC, Farrell GC. Pharmacological cholesterol lowering reverses fibrotic NASH in obese, diabetic mice with metabolic syndrome. Journal of hepatology. 2013; 59:144–152. [PubMed: 23500152]
40. Van Rooyen DM, Larter CZ, Haigh WG, Yeh MM, Ioannou G, Kuver R, Lee SP, Teoh NC, Farrell GC. Hepatic free cholesterol accumulates in obese, diabetic mice and causes nonalcoholic steatohepatitis. Gastroenterology. 2011; 141:1393–1403. 1403 e1391–1395. [PubMed: 21703998]
41. West KL, Zern TL, Butteiger DN, Keller BT, Fernandez ML. SC-435, an ileal apical sodium co-dependent bile acid transporter (ASBT) inhibitor lowers plasma cholesterol and reduces atherosclerosis in guinea pigs. Atherosclerosis. 2003; 171:201–210. [PubMed: 14644388]
42. Dawson PA, Haywood J, Craddock AL, Wilson M, Tietjen M, Kluckman K, Maeda N, Parks JS. Targeted deletion of the ileal bile acid transporter eliminates enterohepatic cycling of bile acids in mice. The Journal of biological chemistry. 2003; 278:33920–33927. [PubMed: 12819193]
43. Mells JE, Fu PP, Kumar P, Smith T, Karpen SJ, Anania FA. Saturated fat and cholesterol are critical to inducing murine metabolic syndrome with robust nonalcoholic steatohepatitis. The Journal of nutritional biochemistry. 2015; 26:285–292. [PubMed: 25577467]
44. Tollefson MB, Kolodziej SA, Fletcher TR, Vernier WF, Beaudry JA, Keller BT, Reitz DB. A novel class of apical sodium co-dependent bile acid transporter inhibitors: the 1,2-benzothiazepines. Bioorganic & medicinal chemistry letters. 2003; 13:3727–3730. [PubMed: 14552767]
45. Kleiner DE, Brunt EM, Van Natta M, Behling C, Contos MJ, Cummings OW, Ferrell LD, Liu YC, Torbenson MS, Unalp-Arida A, Yeh M, McCullough AJ, Sanyal AJ. N. Nonalcoholic Steatohepatitis Clinical Research. Design and validation of a histological scoring system for nonalcoholic fatty liver disease. Hepatology. 2005; 41:1313–1321. [PubMed: 15915461]
46. Reddy GK, Enwemeka CS. A simplified method for the analysis of hydroxyproline in biological tissues. Clinical biochemistry. 1996; 29:225–229. [PubMed: 8740508]
47. Hagio M, Matsumoto M, Fukushima M, Hara H, Ishizuka S. Improved analysis of bile acids in tissues and intestinal contents of rats using LC/ESI-MS. Journal of lipid research. 2009; 50:173–180. [PubMed: 18772484]
48. Langmead B, Trapnell C, Pop M, Salzberg SL. Ultrafast and memory-efficient alignment of short DNA sequences to the human genome. Genome biology. 2009; 10:R25. [PubMed: 19261174]

49. Gentleman RC, Carey VJ, Bates DM, Bolstad B, Dettling M, Dudoit S, Ellis B, Gautier L, Ge Y, Gentry J, Hornik K, Hothorn T, Huber W, Iacus S, Irizarry R, Leisch F, Li C, Maechler M, Rossini AJ, Sawitzki G, Smith C, Smyth G, Tierney L, Yang JY, Zhang J. Bioconductor: open software development for computational biology and bioinformatics. Genome biology. 2004; 5:R80. [PubMed: 15461798]

50. Wu H, Wang C, Wu Z. A new shrinkage estimator for dispersion improves differential expression detection in RNA-seq data. Biostatistics. 2013; 14:232–243. [PubMed: 23001152]

51. Huang da W, Sherman BT, Lempicki RA. Systematic and integrative analysis of large gene lists using DAVID bioinformatics resources. Nature protocols. 2009; 4:44–57. [PubMed: 19131956]

52. Kosters A, White DD, Sun H, Thevananther S, Karpen SJ. Redundant roles for cJun-N-terminal kinase 1 and 2 in interleukin-1beta-mediated reduction and modification of murine hepatic nuclear retinoid X receptor alpha. Journal of hepatology. 2009; 51:898–908. [PubMed: 19767119]

53. Kosters A, Tian F, Wan YJ, Karpen SJ. Gene-specific alterations of hepatic gene expression by ligand activation or hepatocyte-selective inhibition of retinoid X receptor-alpha signalling during inflammation. Liver international : official journal of the International Association for the Study of the Liver. 2012; 32:321–330. [PubMed: 22098603]

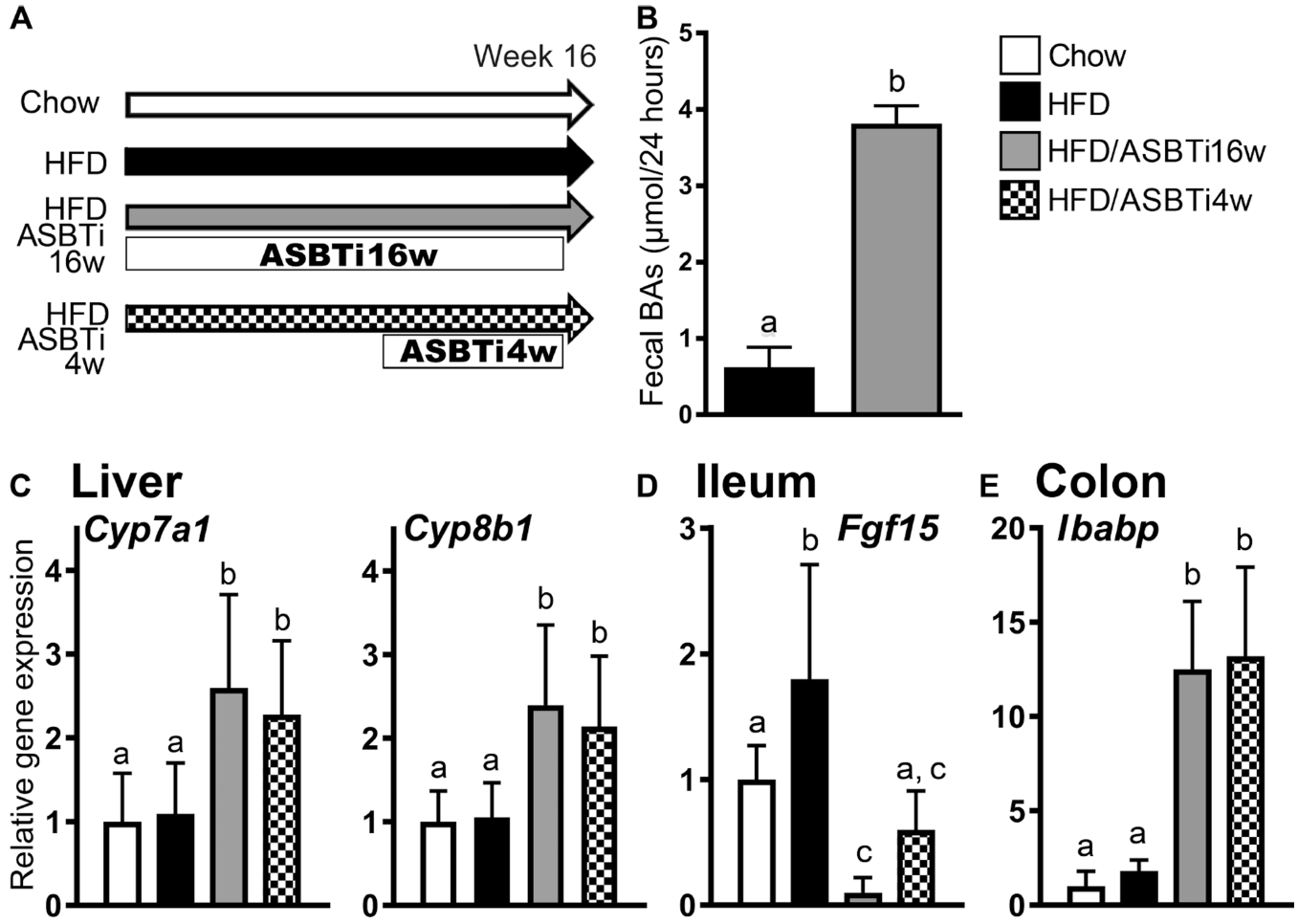

Fig. 1. Administration of an ASBTi increases fecal BA excretion and hepatic BA synthesis

(**A**) Study design showing diets and durations of ASBTi (SC-435) treatments: chow (n=12), HFD (n=12), HFD/ASBTi16w (n=16), HFD/ASBTi4w (n=8). (**B**) Fecal BA excretion in HFD and HFD/ASBTi16w feeding groups. (**C**) Hepatic expression of *Cyp7a1* and *Cyp8b1* mRNA. (**D**) Ileal *Fgf15* mRNA expression and (**E**) colonic *Ibabp* mRNA expression. The labeling scheme for each group is indicated in the embedded legend. Mean ± SD are shown. Distinct lowercase letters indicate significant differences between groups; individual *P* values are provided in table S1.

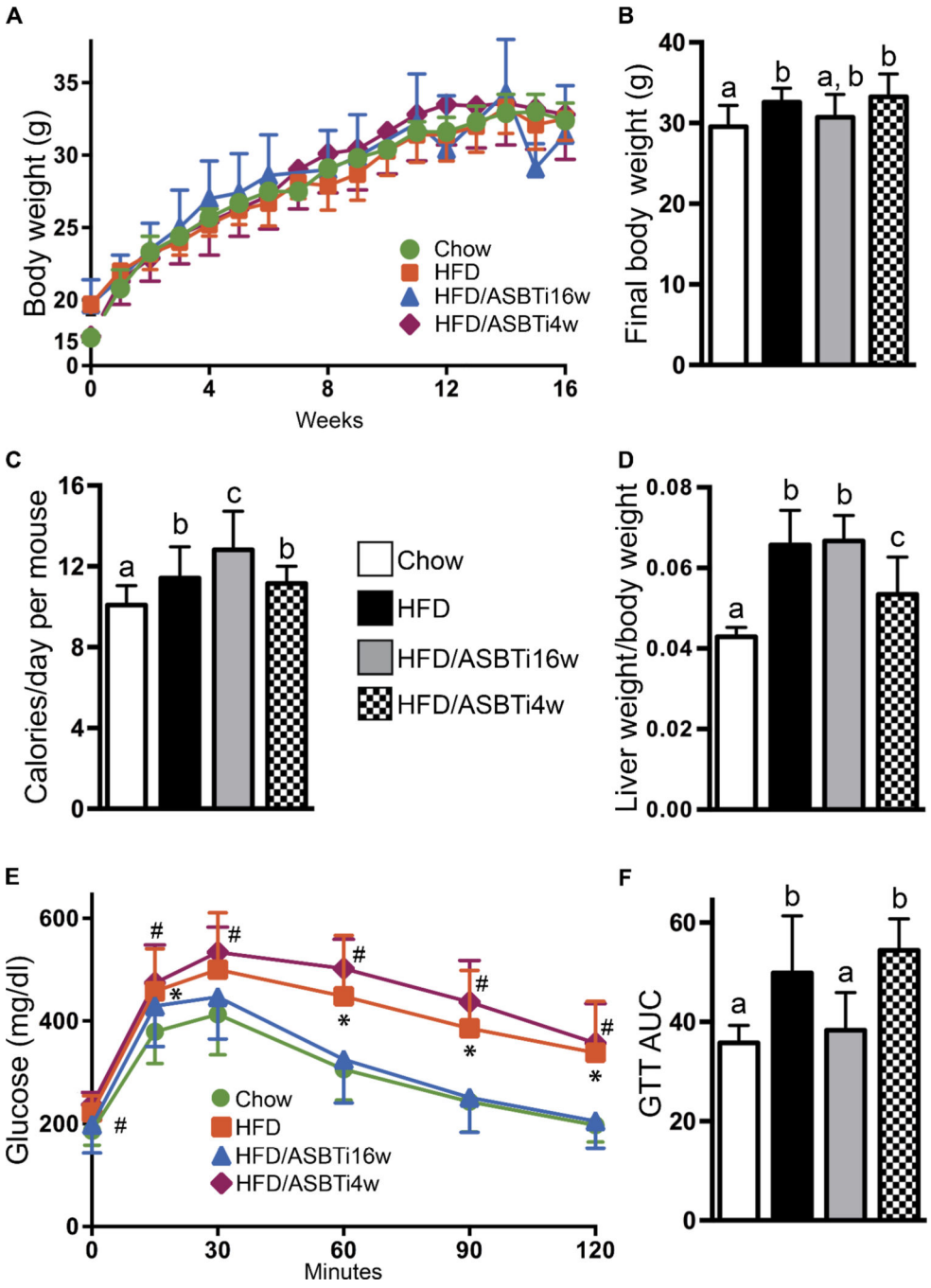

Fig. 2. Administration of an ASBTi restores glucose tolerance

(**A**) Body weight gain in the indicated ad libitum-fed groups. (**B**) Final body weight. (**C**) Average caloric intake over 16 weeks of ad-libitum feeding. (**D**) Liver: body weight ratio after 16 weeks. (**E**) Glucose tolerance tests (GTTs). (**F**) GTT area under the curve (AUC) (g per liter per min). The labeling scheme for each group is indicated in the embedded legend. Mean ± SD are shown. Distinct lowercase letters indicate significant differences between groups). In panel (**E**), * indicates values significantly different between chow and HFD, #

indicates values significantly different between chow and HFD/ASBTi4w; individual *P* values are provided in table S1.

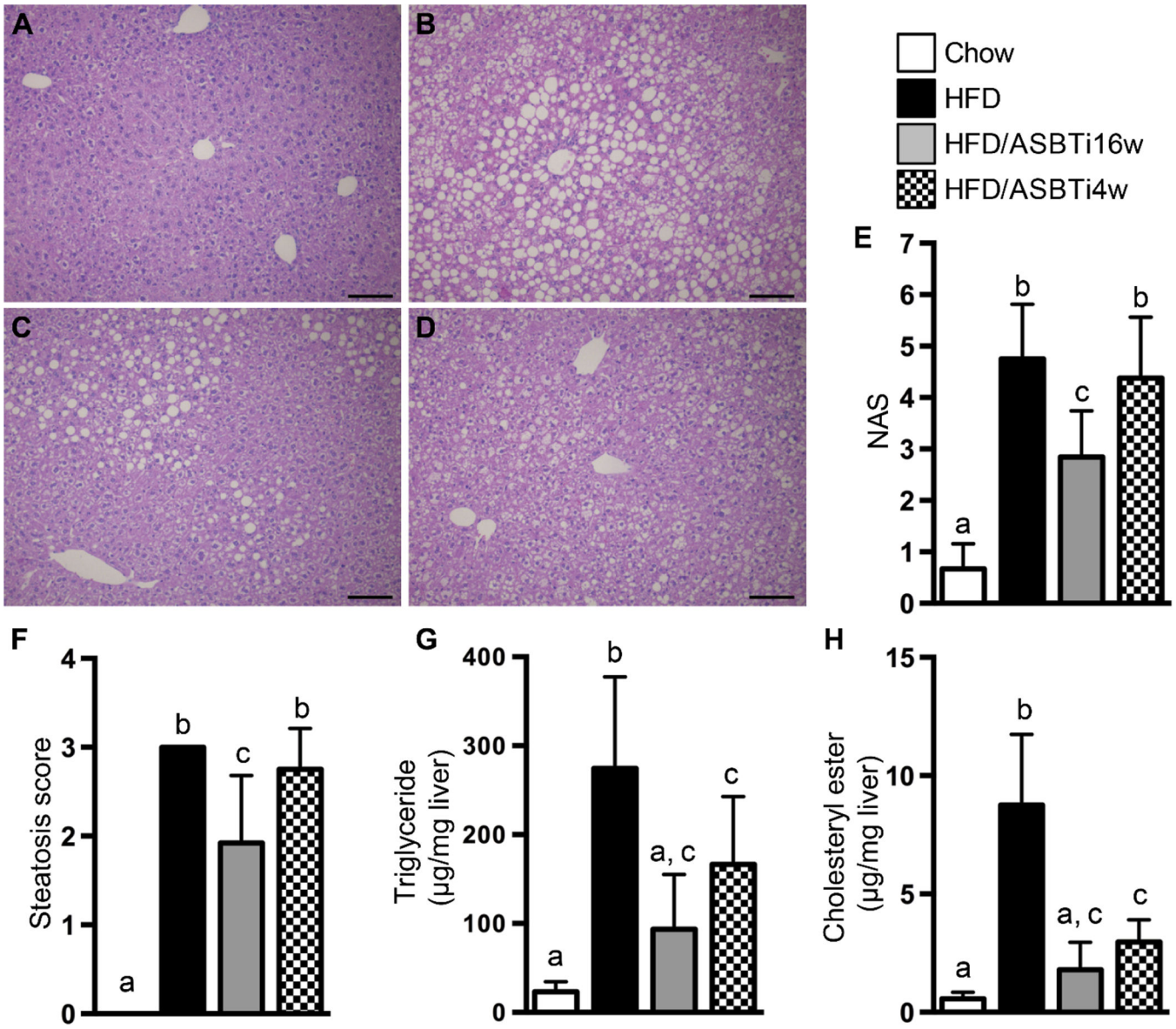

Fig. 3. Administration of an ASBTi reduces hepatic steatosis and accumulation of TGs and cholesterol

Hematoxylin and eosin-stained liver sections from (**A**) chow, (**B**) HFD, (**C**) HFD/ASBTi16w, and (**D**) HFD/ASBTi4w fed mice. (**E**) NAS. (**F**) Steatosis score. (**G**) Hepatic TG content. (**H**) Hepatic cholesteryl ester content. The labeling scheme for each group is indicated in the embedded legend. Mean ± SD are shown. Different lowercase letters indicate significant differences between groups; individual *P* values are provided in table S1. Size bar in panels A to D corresponds to 100 μm.

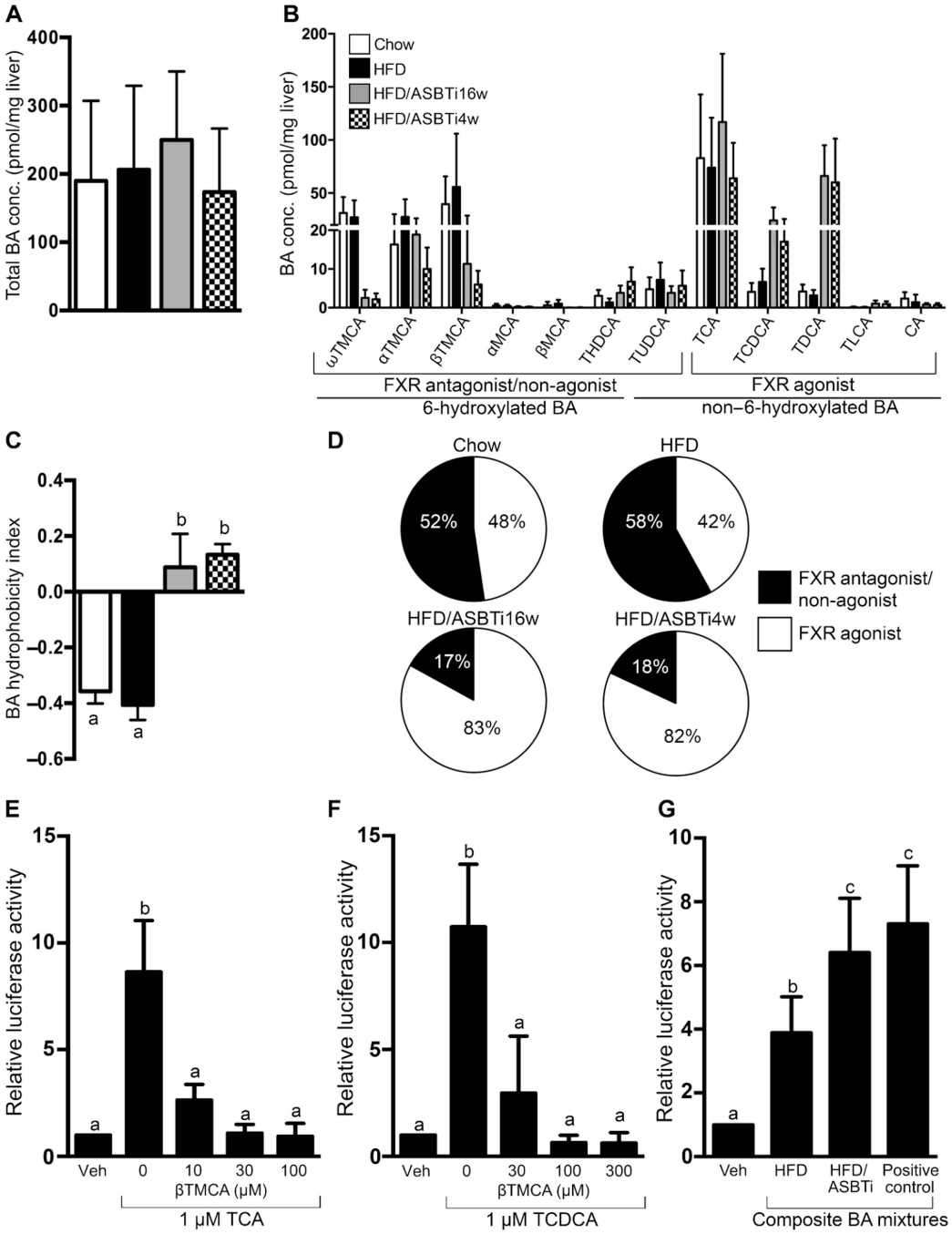

Fig. 4. Administration of an ASBTi shifts hepatic BA composition towards FXR agonism

(**A**) Total hepatic BA content and (**B**) composition (TMCA, tauromuricholic acid; MCA, muricholic acid, THDCA, taurohyodeoxycholic acid; TUDCA, tauroursodeoxycholic acid; TCA, taurocholic acid; TCDCA, taurochenodeoxycholic acid; TDCA, taurodeoxycholic acid; TLCA, taurolithocholic acid; CA, cholic acid). (**C**) Hydrophobicity index. (**D**) Pie charts for hepatic FXR antagonist/non-agonist (black) and agonist (white) BA content. (**E**) βTMCA inhibits TCA-induced FXR activation in HepG2 cells. (**F**) βTMCA inhibits TCDCA-induced FXR activation in HepG2 cells. The concentration of the individual BAs is

indicated on the X-axis. (**G**) Activation of an FXR reporter plasmid (pECRELuc) in transfected HepG2 cells by composite mixtures of the 6 major BAs (3 μM final concentration) modeling the in vivo hepatic BA content from the indicated groups. The vehicle (Veh) used was methanol and positive control consisted of 3 μM TCDCA. The composition of the BA mixtures used in these in vitro studies is shown in table S3. The labeling scheme for each group is indicated in the embedded legend. Mean ± SD are shown. Distinct lowercase letters indicate significant differences between groups; individual *P* values are provided in table S1.

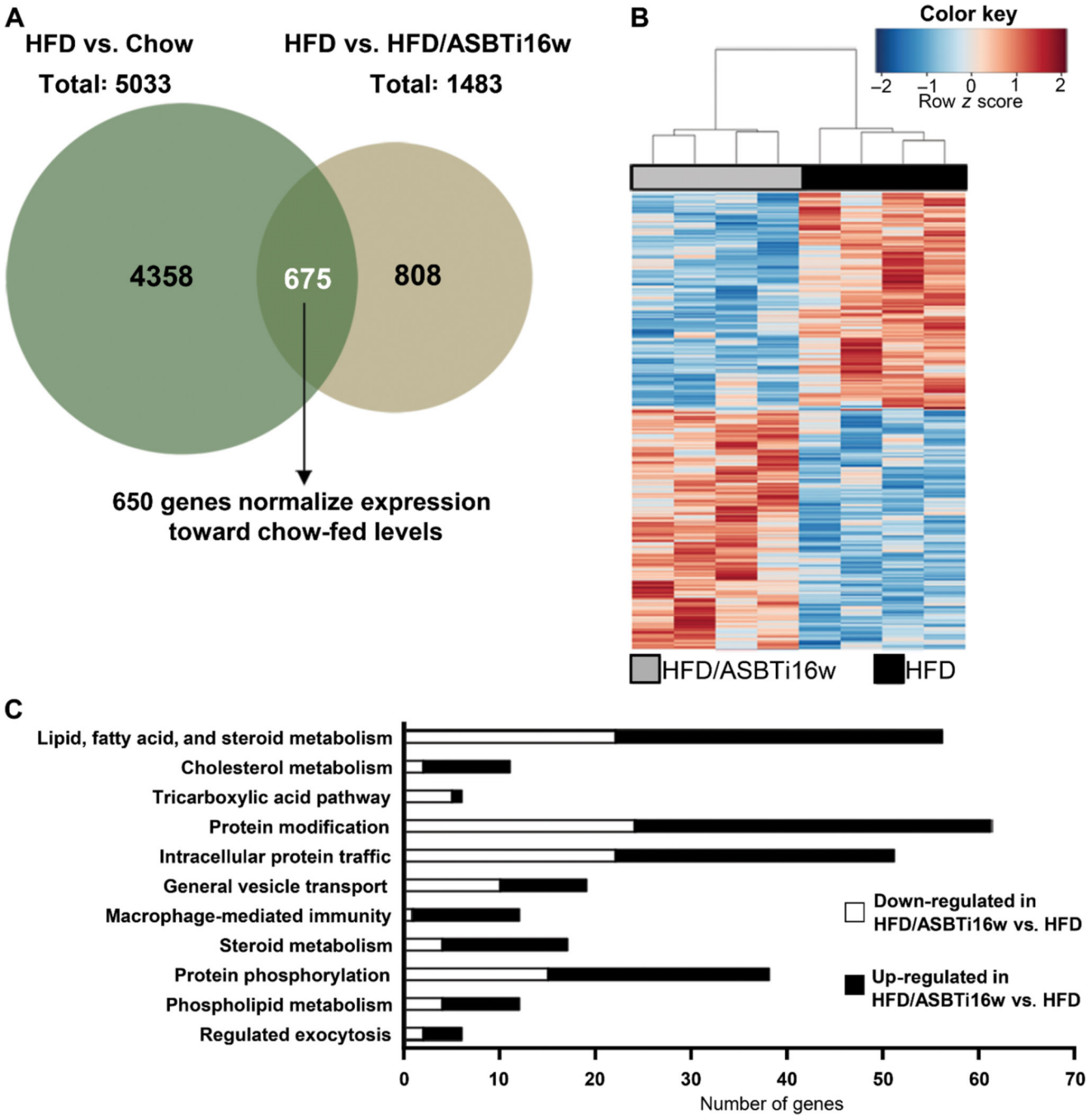

Fig. 5. Inhibition of ileal ASBT function alters global hepatic gene expression

(**A**) Venn diagram of RNA-seq analysis of the two comparisons: HFD vs. Chow and HFD vs. HFD/ASBTi16w. (**B**) Heat map comparing liver gene expression in HFD vs HFD/ASBTi16w groups. (**C**) Ontology analysis/pathway (Panther) analysis of HFD vs HFD/ASBTi16w as downregulated (white bars) and upregulated (black bars) pathways.

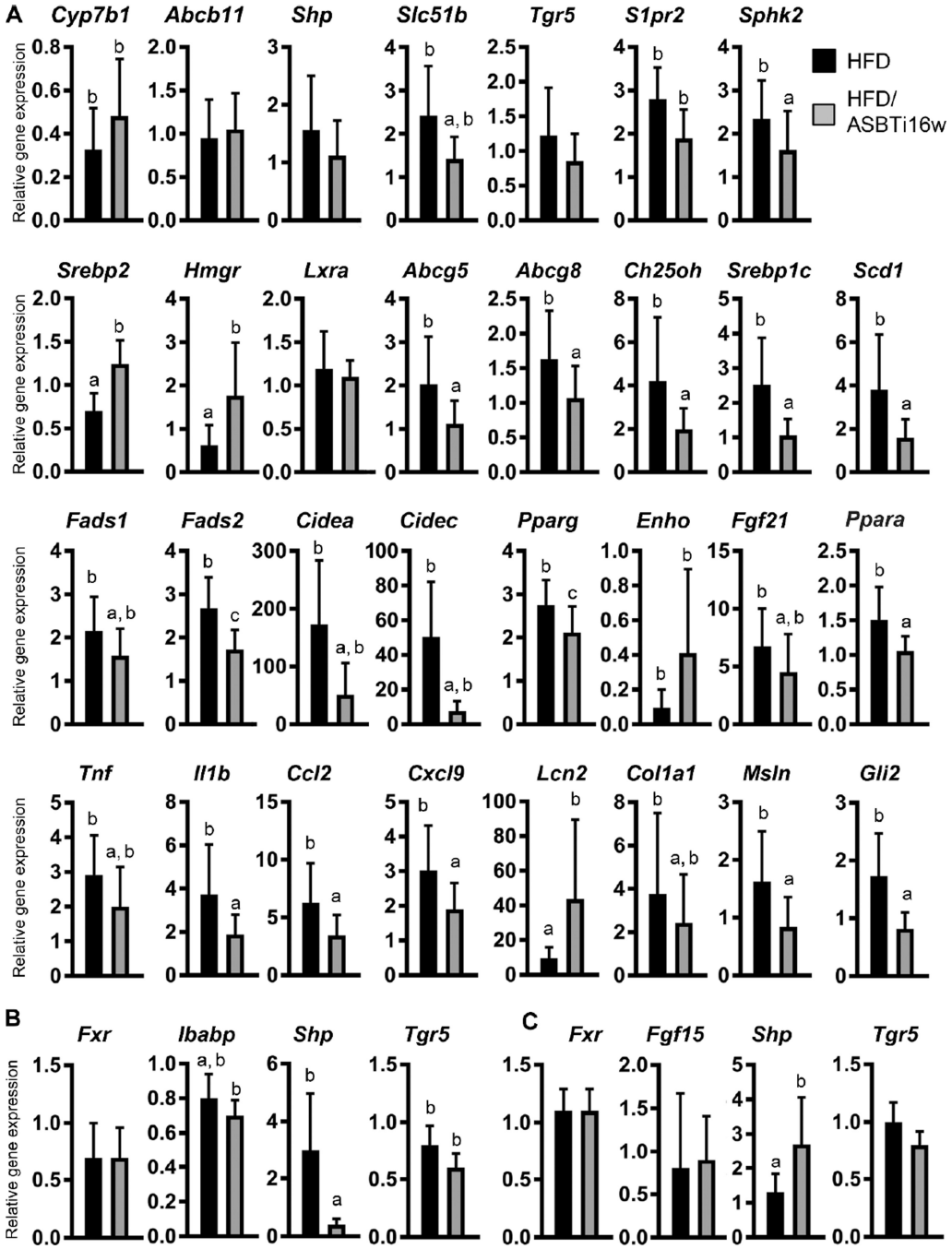

Fig. 6. Administration of an ASBTi alters hepatic and intestinal gene expression

(**A**) Hepatic mRNA expression of genes involved in BA signaling and transport, cholesterol synthesis, lipid synthesis, lipid droplet formation, fatty acid oxidation, inflammation, and fibrosis. (**B**) mRNA expression of genes involved in BA signaling and transport in the ileum and (**C**) colon. Quantitative real-time PCR was performed on chow, HFD, HFD/ASBTi16w, and HFD/ASBTi4w groups, and expression shown relative to chow (set as 1). For clarity, gene expression in the HFD and HFD/ASBTi16w groups are displayed. Cyclophilin was used as a housekeeping gene to normalize mRNA expression. The labeling scheme for each

group is indicated in the embedded legend. Mean ± SD are shown. Distinct lowercase letters indicate significant differences between groups; individual *P* values are provided in table S1.

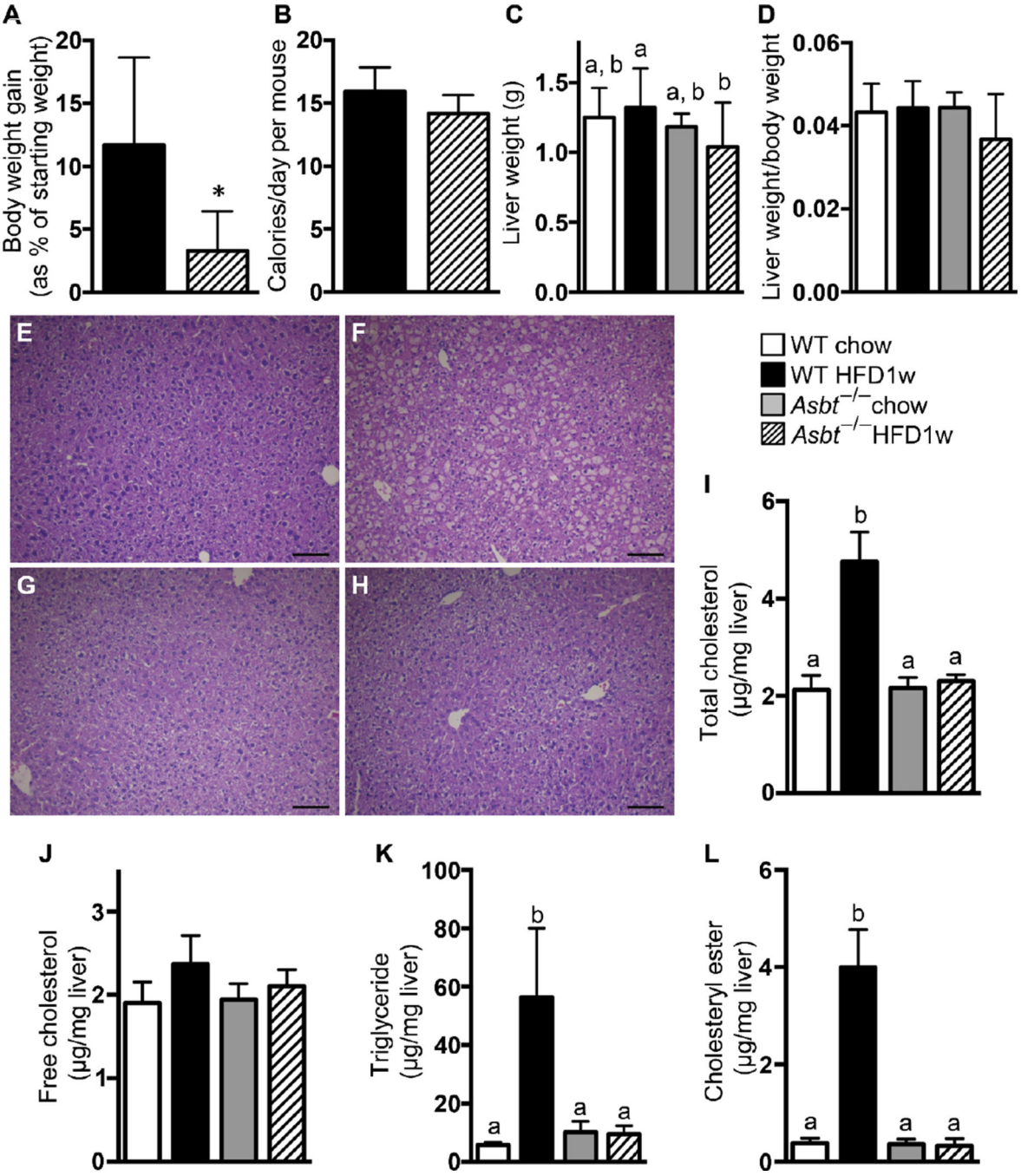

Fig. 7. Hepatic accumulation of TGs and cholesterol is reduced in *Asbt*$^{-/-}$ mice

(**A**) Body weight gain in the indicated ad libitum-fed groups. (**B**) Average caloric intake over 1 week of feeding. (**C**) Liver weight after 1 week of HFD or chow. (**D**) Liver:body weight ratio after 1 week of HFD or chow. Hematoxylin and eosin-stained liver sections from (**E**) WT/chow, (**F**) WT/HFD 1 week, (**G**) *Asbt*$^{-/-}$/Chow, and (**H**) *Asbt*$^{-/-}$/HFD 1 week mice. (**I**) Hepatic total cholesterol content. (**J**) Hepatic free cholesterol content. (**K**) Hepatic TG content. (**L**) Hepatic cholesteryl ester content. The labeling scheme for each group is indicated in the embedded legend. Mean ± SD are shown. Distinct lowercase letters indicate

significant differences between groups; individual *P* values are provided in table S1. Size bar in panels E to H corresponds to 100 μm.

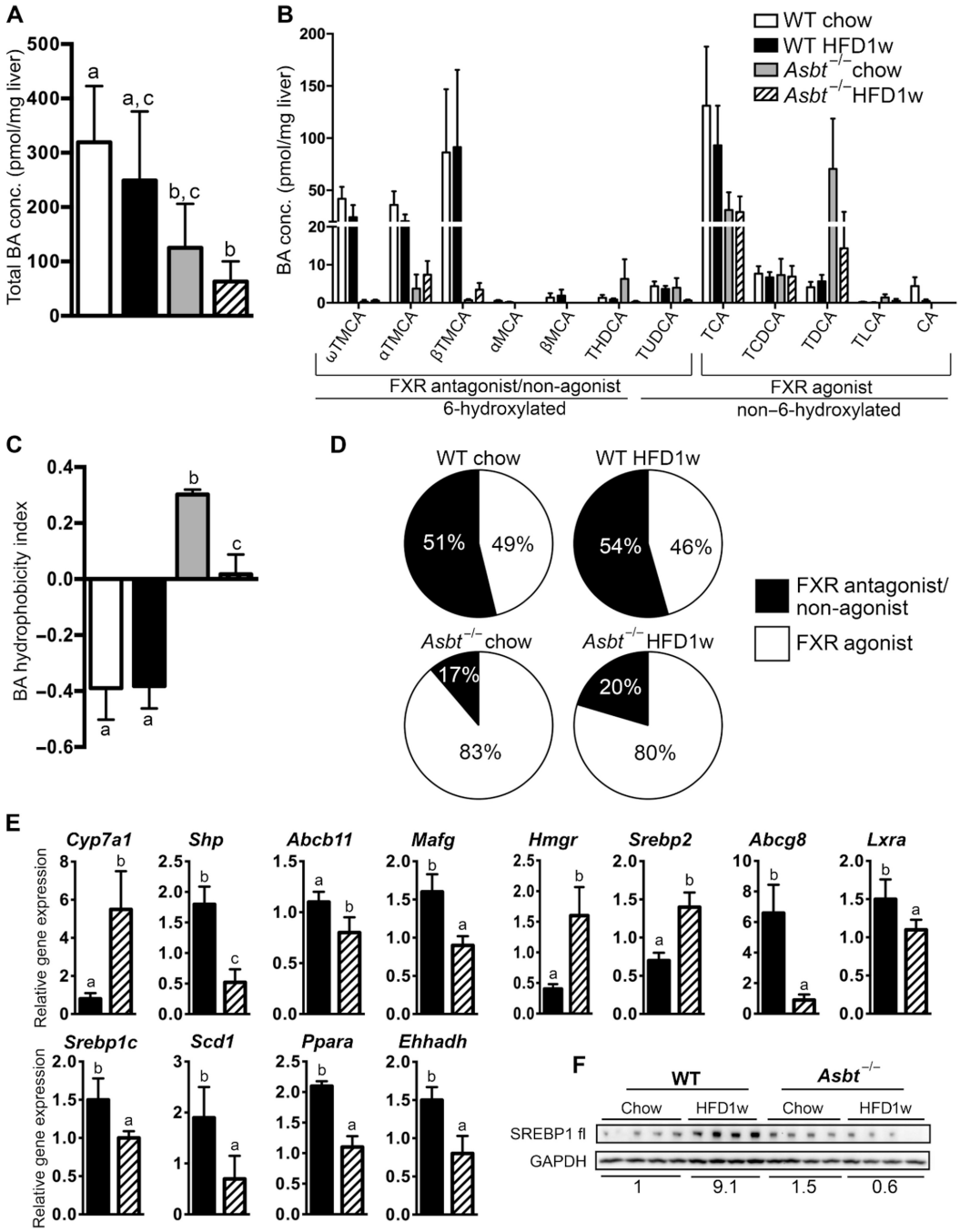

Fig. 8. Hepatic BA composition is altered in *Asbt*$^{-/-}$ mice

(**A**) Total hepatic BA content and (**B**) BA composition. (**C**) Hydrophobicity index and (**D**) Pie charts for hepatic FXR antagonist/non-agonist (black) and agonist (white) BA content. (**E**) Hepatic gene expression in WT and *Asbt*$^{-/-}$ mice fed a HFD for 1 week. Values shown are relative to chow-fed WT mice. (**F**) Protein expression of full-length (fl) SREBP1 increased in HFD-fed WT mice but not in HFD-fed *Asbt*$^{-/-}$ mice. SREBP1 expression was normalized to the amount of the housekeeping protein GAPDH and the quantitation is shown below the blot. The labeling scheme for each group is indicated in the embedded

legend. Mean ± SD are shown. Distinct lowercase letters indicate significant differences between groups; individual *P* values are provided in table S1.